JACS
JOURNAL OF THE AMERICAN CHEMICAL SOCIETY
Article
Cite This: J. Am. Chem. Soc. 2019, 141, 14772−14779
pubs.acs.org/JACS

Synergistic Effect of High-Frequency Ultrasound with Cupric Oxide Catalyst Resulting in a Selectivity Switch in Glucose Oxidation under Argon

Prince N. Amaniampong,[†,○] Quang Thang Trinh,[‡,§,○] Karine De Oliveira Vigier,[∥] Duy Quang Dao,[§] Ngoc Han Tran,[⊥] Yingqiao Wang,[#] Matthew P. Sherburne,[*,#,▽] and François Jérôme[*,†,∥]

[†]CNRS Research Federation INCREASE, 1 Rue Marcel Doré, TSA 41105, 86073 Poitiers, France

[‡]Cambridge Centre for Advanced Research and Education in Singapore (CARES), Campus for Research Excellence and Technological Enterprise (CREATE), 1 Create Way, 138602 Singapore

[§]Institute of Research and Development, Duy Tan University, 03 Quang Trung, Danang 550000, Viet Nam

[∥]Institut de Chimie des Milieux et Matériaux de Poitiers (IC2MP), Université de Poitiers, CNRS, 1 Rue Marcel Doré, TSA 41105, 86073 Poitiers, France

[⊥]NUS Environmental Research Institute, National University of Singapore, 5A Engineering Drive 1, T-Lab Building, 117411 Singapore

[#]Materials Science and Engineering Department, University of California, Berkeley, Berkeley, California 94720, United States

[▽]Singapore Berkeley Research Initiative for Sustainable Energy, Berkeley Educational Alliance for Research in Singapore (BEARS), 1 Create Way, 138602 Singapore

Supporting Information

ABSTRACT: We report here, and rationalize, a synergistic effect between a non-noble metal oxide catalyst (CuO) and high-frequency ultrasound (HFUS) on glucose oxidation. While CuO and HFUS are able to independently oxidize glucose to gluconic acid, the combination of CuO with HFUS led to a dramatic change of the reaction selectivity, with glucuronic acid being formed as the major product. By means of density functional theory (DFT) calculations, we show that, under ultrasonic irradiation of water at 550 kHz, the surface lattice oxygen of a CuO catalyst traps H· radicals stemming from the sonolysis of water, making the ring-opening of glucose energetically unfavorable and leaving a high coverage of ·OH radical on the CuO surface, which selectively oxidizes glucose to glucuronic acid. This work also points toward a path to optimize the size of the catalyst particle for an ultrasonic frequency that minimizes the damage to the catalyst, resulting in its successful reuse.

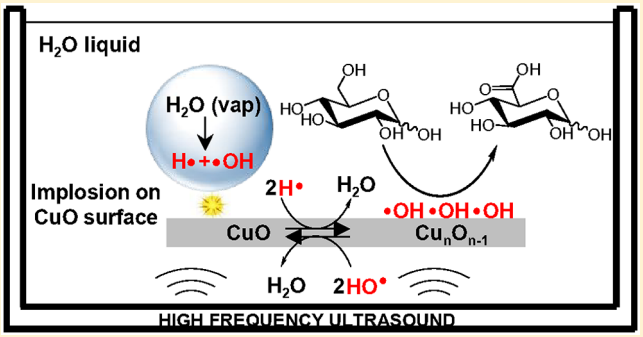

INTRODUCTION

Glucuronic acid is an important chemical for both social and industrial reasons; for example, it plays a crucial role in the detoxification of drugs and toxins. Glucuronic acid is a promising intermediate in the fledgling, but fast-growing, renewable chemical industry, allowing the synthesis of chemicals with improved performances. For instance, glucuronic acid is a key precursor in the synthesis of proteoglycans, glycoglycerolipids, ascorbic acid, surfactants, and monomers such as glucaric and adipic acids used in the fabrication of renewably sourced polymers.[1,2] The selective oxidation of glucose to glucuronic acid (oxidation at the C6 position) remains a formidable challenge in the field of catalysis. Indeed, most of the catalysts, including noble and non-noble metal catalysts in combination with oxygen or hydrogen peroxide, oxidize glucose at the anomeric position (oxidation at the C1 position), leading to the formation of gluconic acid instead of glucuronic acid (Scheme 1).[3−8] To circumvent this problem, the anomeric position of glucose is protected by Fisher glycosylation,[9] acetalization,[10] or reaction with phosphate groups[11] prior to the oxidation of the C6 position, followed by deprotection of the C1 position. Wojcieszak and co-workers[12] reported one of the rare examples of selective oxidation of unprotected glucose to glucuronic acid (53% yield), using hydrazine-neutralized basic cesium-promoted

Received: July 3, 2019
Published: August 27, 2019

DOI: 10.1021/jacs.9b06824
J. Am. Chem. Soc. 2019, 141, 14772−14779

Scheme 1. Contribution of This Work to the State of the Art

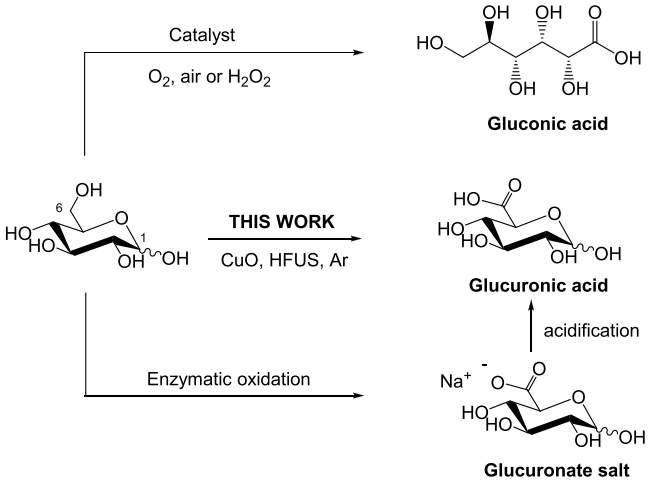

gold nanoparticles as a catalyst. However, the reaction mechanism and the origin for this unexpected selectivity were not reported. In other work reporting on the catalytic oxidation of glucose, low selectivity to glucuronic acid (<5%) was always observed.[13,14] In the current state of the art, glucuronic acid is produced by fermentation routes that produce glucuronate salt, thus requiring an extra acidification step (Scheme 1).[2] The development of alternative catalytic technologies capable of selectively oxidizing unprotected glucose to glucuronic acid is an important scientific challenge that is addressed in this work.

When water is subjected to an ultrasonic irradiation at a high frequency (100−800 kHz), small gaseous cavitation bubbles are formed (<10 μm) that contain a sufficient amount of energy to dissociate water to H· and ·OH radicals.[15] On implosion of the cavitation bubbles, radicals are propelled into the bulk solution, where they react with organic solutes. The selectivity of the resulting radical reactions is quite difficult to control, and, for this reason, high-frequency ultrasound (HFUS) is mainly used for the total free oxidation of aqueous pollutants.[16] The ability to control the selectivity of these radical oxidative reactions is highly desirable to the implementation of this technology to the synthesis of a variety of chemicals, such as glucuronic acid, but it remains an elusive task. One solution consists of the introduction of a catalyst during the ultrasonic irradiation. This strategy, coined sonocatalysis, has been previously explored, with the focus being mostly on low-frequency ultrasound (<20 kHz), i.e., the formation of radicals was very low and mainly physical effects occur. In this case, the turbulent flow and shock waves produced by the implosion of cavitation bubbles improve the dispersion of catalyst/reactant and the mass transfer and, sometimes, prevent the catalyst from coking, resulting in improved reaction rates.[17] For instance, this strategy has been explored to accelerate the iron-catalyzed oxidation rate of glucose with hydrogen peroxide, but, as expected, it yields gluconic acid as the main reaction product.[18] To the best of our knowledge, controlling the selectivity of radical reactions induced by HFUS with the help of solid catalysts has not been reported yet. To optimize the reaction selectivity, in situ produced radicals by HFUS should interact faster with the catalyst surface than with organic solutes present in the bulk solution. In a heterogeneous solution, the formation of cavitation bubbles occurs preferentially on the particle surface via heterogeneous nucleation.[19−22] In contrast to homogeneous solution, implosion of cavitation bubbles on a solid surface thus generates high-speed jets of liquid directed toward the surface. It occurred to us that this physical behavior could be a means to greatly increase selective transfer of radicals produced inside the cavitation bubble to a solid catalyst surface, thus allowing better control of the reaction selectivity.

Recently, we reported the catalyst-free oxidation of glucose induced by HFUS.[23] Surprisingly, the selectivity of the reaction was significantly impacted by the nature of the gaseous atmosphere. Under Ar, gluconic acid was formed as a major product, while under O_2, glucuronic acid was formed in a significant amount. Our efforts to rationalize this difference of selectivity, and inspired by our previous investigations in catalytic oxidation,[8,24] led us to discover a synergistic effect between CuO and HFUS on the glucose oxidation. While CuO and HFUS are able to independently oxidize glucose to gluconic acid under argon, the combination of CuO with HFUS led to a complete reversal of the reaction selectivity, with glucuronic acid being formed as the major product. Through a combined experimental-theoretical approach, we rationalize here the synergistic effect between CuO and HFUS on glucose oxidation. In particular, we show that, under ultrasonic irradiation of water at a high frequency (550 kHz), the surface lattice oxygen of a CuO catalyst traps H· radicals stemming from the sonolysis of water, eliminating the participatory role of H· in the ring-opening of glucose and favoring the selective oxidation of glucose to glucuronic acid. We also highlight that the particle size of CuO is an important parameter governing an optimal transfer of radicals from the cavitation bubbles to the catalyst surface.

RESULTS AND DISCUSSION

In line with our previous report, under argon, the catalyst-free ultrasonic irradiation of an aqueous solution of glucose at high frequency (550 kHz, 40 °C) led to the formation of gluconic acid (55% yield) as a major product.[23] DFT calculations performed at a M05-2X/6-311++G(d,p) level of theory[25] using the Gaussian DFT code[26] confirmed the preferential oxidation of the anomeric position (calculated on the glucopyranose form predominantly existing in water). The generation of H· and ·OH radicals, as a consequence of cavitation bubbles collapse, favors the ring-opening of glucose and follows a widely accepted concerted mechanism: (1) abstraction of the H atom at the anomeric position by the ·OH radical (E_a = 1.1 kJ/mol, TS1a (TS = transition state) in Figure 1), forming water, and (2) a very energetically favorable addition of H· radical on the oxygen atom of the ring (ΔE = −499.8 kJ/mol, Int1b to Int2b in Figure 1), which induced the ring-opening. The dehydrogenation on the C6 position of glucose is also a feasible reaction, but with a higher activation energy barrier (E_a = 14 kJ/mol[23]) than the ring-opening path. Interestingly, without assistance of H· radicals, the ring-opening of glucose becomes significantly less favorable energetically (E_a = 114.2 kJ/mol, TS2a in Figure 1) than the oxidation on the C6 position of glucose. Hence, we hypothesize that if H· radicals are completely suppressed (i.e., only ·OH radicals remain) during the sonolysis of water, then glucose should be selectively oxidized to glucuronic acid.

Previous studies have reported that ·OH radicals bound to the CuO surface via the bridge sites between two undercoordinated surface lattice Cu_3 atoms, while H· radicals adsorb strongly on top of the undercoordinated lattice oxygen sites on

DOI: 10.1021/jacs.9b06824
J. Am. Chem. Soc. 2019, 141, 14772−14779

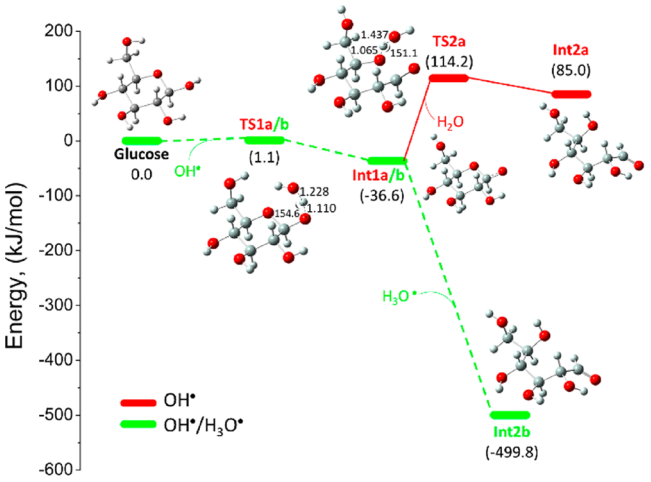

Figure 1. Potential energy profiles for glucose ring-opening reaction in vacuum calculated at the M05-2*X*/6-311++G(d,p) level of theory facilitated by HO• and HO•/ H_3O• radicals (H• + H_2O). Label of structure: Int, intermediate compounds; TS, transition state. Key structural parameters for the transition states including bond lengths in Å, and angles in degree are indicated.

the surface of CuO.[24,27−30] Adsorbed H· radicals have a diffusion barrier of 0.53 eV,[31] allowing migration and the reaction with lattice oxygen to form H_2O with a reaction energy of −0.82 eV.[28] This process then results in generating an oxygen vacancy at the CuO surface,[8,24,30] and a surface of CuO covered by ·OH radicals, as reported by Bhola et al.[27] and Song and Wang.[31] From these results, a reasoned approach suggested that the association of CuO catalyst with HFUS should be a viable strategy to in situ trap the radical H·, which would inhibit the ring-opening of glucose and, thus, would shift the selectivity of the oxidation reaction toward glucuronic acid.

Unless otherwise noted, CuO used in this work was prepared according to our previously reported methodology[24] (see the Supporting Information for more details on CuO characterization). In agreement with DFT calculations, when CuO was introduced during the ultrasonic irradiation of an aqueous solution of glucose under argon (550 kHz, 80 °C), the selectivity of the reaction was changed and glucuronic acid was now obtained as a major product, with 66% yield. A similar trend was observed when other hexoses such as mannose and galactose were tested under the same experimental conditions. In these cases, the corresponding uronic acids were obtained with 70% and 64% yields from mannose and galactose, respectively. CuO catalytic material can be up to 10 wt % without affecting the reaction selectivity, suggesting that CuO can be used in a catalytic amount and was therefore in situ reoxidized under HFUS conditions (discussed later in the text). The in situ regeneration of CuO was confirmed by X-ray diffraction (XRD) analysis, with XRD patterns of the spent CuO being rigorously studied, and showed similar patterns to those of the fresh CuO (Figure S1a and b).

To obtain additional data, the catalytic reaction was performed under silent conditions (i.e., 80 °C, under Ar, without HFUS). Under argon, CuO reacted with glucose in a stoichiometric way, leading to the formation of gluconic acid instead of glucuronic acid. This oxidation under silent conditions occurs through the insertion of surface lattice oxygen from CuO into the glucose, resulting in a partial reduction of CuO to Cu_nO_{n-1}, as confirmed by XRD analysis (Figure S1c) (i.e., Mars−Krevelen-type mechanism). On the basis of the gluconic acid yield, we determined that ∼93% of the oxygen of CuO was consumed by glucose in this case (a value in line with a previous work of Amaniampong et al.[8]) The oxidation mechanism of glucose to gluconic acid over bare CuO is discussed later in this Article. When this partly reduced CuO was then treated by HFUS (50 mL of water, 80 °C, 550 kHz), XRD analysis unambiguously confirmed that CuO was in situ reoxidized under HFUS conditions (Figure S4). The DFT calculations we performed confirm that the reoxidation of CuO by ·OH radicals is a favorable energetic reaction (ΔE = −66 kJ/mol).

To rationalize this synergistic effect between HFUS and CuO, we performed calculations with the periodic plane-wave implementation of DFT using VASP (Vienna ab initio simulation package).[32−34] Under HFUS conditions, the surface of CuO is covered by ·OH radicals. Without HFUS, the water splitting of H_2O on Cu(111) of CuO is energetically unfavorable (132 kJ/mol),[8] and, in this case, the bare CuO surface was computed.

First the oxidation of glucose to gluconic acid was investigated, with the ring-opening of glucose being the key step;[35] energy profiles are shown in Figure 2. The first step of

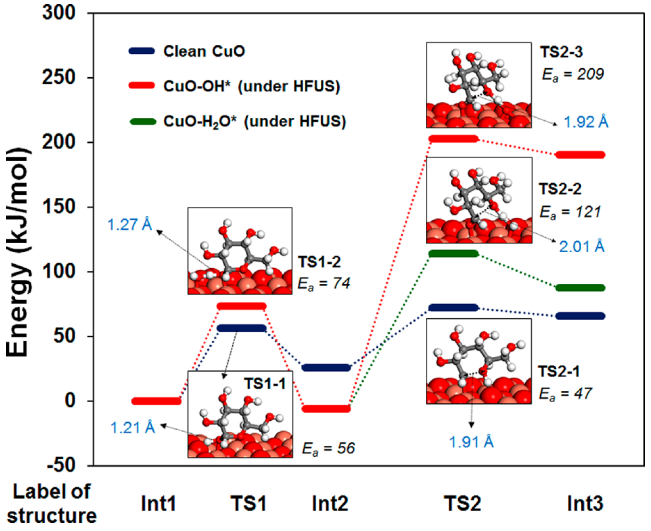

Figure 2. Energy profile for glucose ring-opening process under different conditions. Label of structure: Int1, adsorbed glucose; Int2, product of first step of OH activation; Int3, adsorbed open-chain glucose; TS1 and TS2, transition states of steps 1 and 2, respectively. Bond lengths in Å for the transition states are indicated. Color code: Large peach and red balls represent copper (Cu) and oxygen (O) atoms of the CuO substrate, respectively, and small white, gray, and red balls represent hydrogen (H), carbon (C), and oxygen (O) atoms of the adsorbates, respectively.

the glucose ring-opening is the dehydrogenation of the hydroxyl attached to the C1 position (TS1 in Figure 2).[35,36] This step is feasible on both the bare CuO surface (barrier of 56 kJ/mol, TS1-1) and on the CuO surface covered by ·OH radicals (HFUS, E_a = 74 kJ/mol, TS1-2). However, the second step (hydrogen transfer to the ring, TS2 in Figure 2) has very different behavior with or without HFUS. On the bare CuO surface, the barrier for this step is 47 kJ/mol (TS2-1). Under HFUS conditions (with high coverage of surface by the hydroxyl group), the barrier to abstract the H· atom from a surface hydroxyl group and transfer back to the ring has an

DOI: 10.1021/jacs.9b06824
J. Am. Chem. Soc. 2019, 141, 14772−14779

extremely high barrier of 209 kJ/mol (TS2-3, Figure 2), due to the endothermic energy of this process. If the hydrogen is abstracted from a surface-adsorbed water molecule, the barrier is lower but still very high at 121 kJ/mol (TS2-2, Figure 2), which is 74 kJ/mol higher than the corresponding step on the bare CuO surface. These high barriers, therefore, largely inhibit the ring-opening of glucose on the CuO surface under HFUS conditions.[37,38] Microkinetic modeling of glucose ring-opening on the bare CuO surface and under HFUS conditions (see Supporting Information for detailed discussion) confirmed that the rate of glucose open-chain formation was reduced to negligible values on CuO with high coverage of surface ·OH (assuming the initial coverage of surface OH is 0.7 monolayer (ML) under HFUS conditions).

Then we investigated the oxidation of glucose to glucuronic acid, on both the bare CuO surface and under HFUS conditions (with the presence of surface HO· group on CuO) (Figure 3). The initial OH activation and the subsequent CH

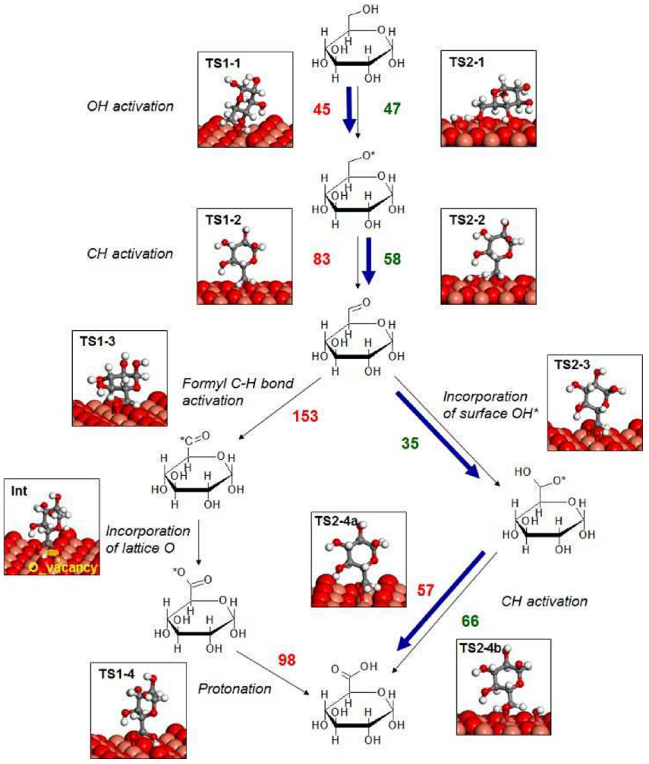

Figure 3. Overall reaction network for the glucose oxidation on CuO surface under HFUS conditions. Two pathways are illustrated. The pathway where reactions are facilitated by surface lattice oxygen of CuO is presented on the left side, and activation barriers are indicated by red color. The pathway where reactions are facilitated by surface OH* group generated under HFUS is presented on the right side, and activation barriers are indicated by green color. The bold blue arrows highlight the more preferred pathway. The color code is the same as the color code used in Figure 2.

dehydrogenation steps from the $-CH_2OH$ group of glucose forming glucose dialdehyde on the bare CuO surface have barriers of 45 kJ/mol (TS1-1) and 83 kJ/mol (TS1-2), respectively, and the reaction is facilitated by the under-coordinated oxygen of CuO(111) surface. These two steps are even more favorable with the surface HO· group present on the CuO surface under HFUS conditions, with the CH dehydrogenation having a relatively low barrier of E_a = 58 kJ/mol, TS2-2.

On the bare CuO surface, the subsequent oxidation of glucose aldehyde requires an activation of the formyl O═C−H bond, which possesses a very high barrier of 153 kJ/mol (TS1-3, Figure 3), making the formation of glucuronic acid very unlikely through this mechanism. Under HFUS conditions, the presence of high coverage surface HO· groups on CuO opens an alternative pathway for glucose oxidation. In this alternative pathway, glucose is oxidized via the incorporation of surface HO· into glucose aldehyde with a barrier of only 35 kJ/mol (TS2-3, Figure 3). This type of reaction has also been proposed and validated for alcohol oxidation on transition metals catalysts.[39,40] After the incorporation of surface HO· group, the formed molecule (Figure 3) undergoes the C−H abstraction either by surface lattice oxygen of CuO (barrier of 57 kJ/mol, TS2-4, Figure 3) or facilitated by adsorbed HO· group on CuO (slightly higher barrier of 66 kJ/mol), generating glucuronic acid as the final product.

To gain insight into the reaction mechanism, the kinetic profile of the reaction was then recorded by plotting the yield of the reaction products as a function of the reaction time (Figure 4). Using 10 wt % of CuO under HFUS, glucuronic

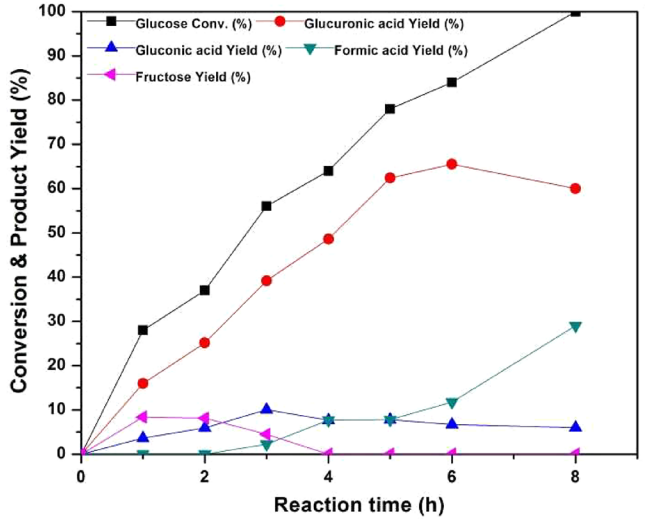

Figure 4. Kinetic profile of the reaction (10 wt % CuO, 80 °C, 550 kHz, glucose concentration 20 g·L^{-1}, P_{acoust} = 0.36 W·mL^{-1}).

acid was formed as a major product (66% yield after 6 h of reaction). Fructose, commonly formed by isomerization of glucose in water, was also detected at the initial stage of the reaction, with a maximum yield of 8% at 28% conversion. The isomerization glucose/fructose is an equilibrated reaction, and fructose is reconverted back to glucose and then glucuronic acid, as illustrated in the kinetic profile by a drop of the fructose yield at conversion >28%. To support this claim, fructose was used as the starting material, affording glucuronic acid with 70% yield. In this case, formation of glucose was also initially observed with a maximum yield of 5% at 50% conversion of fructose (see Supporting Information for detailed kinetics).

Gluconic acid was also detected as a coproduct, albeit in a low amount (yield <10%) (Figure 4). The side formation of gluconic acid may result from diffusion of H· and ·OH radicals

DOI: 10.1021/jacs.9b06824
J. Am. Chem. Soc. 2019, 141, 14772−14779

into the bulk solution, leading to unwanted oxidation of glucose to gluconic acid. When the catalyst loading was varied from 5 to 60 wt %, the formation of gluconic acid was decreased but not completely inhibited, suggesting that the transfer of radicals produced by cavitation bubbles to the CuO surface is not optimal (Figure S5). The heterogeneous nucleation of cavitation bubbles on a material surface is affected by the particle size.[20] A particle with large surface area (lower particle size) favors efficient nucleation and growth of the cavitation bubble, owing to enhanced cavitation bubble–solid particles contact angles.[20] In this context, the present HFUS reactor was employed to prepare CuO, hereafter named CuO_{HFUS}, using our previously reported strategy (sonication of an alkaline solution of $CuNO_3$).[24] Using the same reactor and ultrasonic frequency for the catalyst preparation and the oxidation of glucose is, in our view, a good strategy to optimize the particle size of CuO to that of the cavitation bubbles and, thus, to maximize the transfer of radicals to the CuO surface. The optimized particle sizes of CuO_{HFUS} (3.5–4.7 μm, 30 m^2/g) are ~4 orders of magnitude lower than those of CuO (10–24 μm, 18 m^2/g) while the shape remained similar as confirmed by scanning electron microscopy (SEM) and transmission electron microscopy (TEM) analysis (Figure S7). Pleasingly, over CuO_{HFUS}, formation of gluconic acid was completely suppressed and glucuronic acid was formed with a maximum yield of 88% (95% selectivity at 93% conversion), confirming that, in this case, radicals selectively transfer to the CuO surface and not into the bulk solution, as observed earlier (Figure 5).

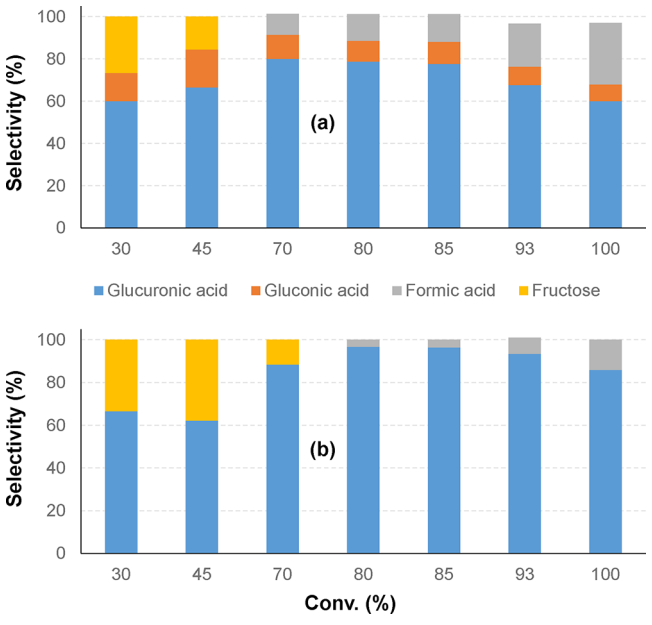

Figure 5. Plot of the selectivity as a function of the conversion of glucose (a) CuO and (b) CuO_{HFUS} (10 wt % copper oxide, 80 °C, 550 kHz, glucose concentration 20 $g{\cdot}L^{-1}$, P_{acoust} = 0.36 $W{\cdot}mL^{-1}$).

At 80 °C, the other detected product was formic acid stemming from the overoxidation of glucose. The formation of formic acid, however, is significantly more important over CuO than over CuO_{HFUS}, a result in line with less efficient cavitation bubble/CuO interactions in the former case. It is noteworthy that, in the presence of CuO_{HFUS}, formic acid was only detected at a conversion >80%, but its formation remained rather low (<10% yield at 93% conversion of glucose, Figure 5b).

As a control reaction, *tert*-butanol, a known radical scavenger in sonochemistry, was added during the reaction.[41] As expected, in this case, radicals were trapped and glucuronic acid was no longer formed. Instead, we observed the classical and stoichiometric oxidation of glucose to gluconic acid (21% yield) by CuO, illustrating the synergistic effect between CuO and HFUS in the selective oxidation of glucose to glucuronic acid.

If the popular low frequency (<20 kHz) is known to damage catalyst, mainly by abrasion resulting from intense shock waves, this phenomenon is much less likely to occur at HFUS for which cavitation bubbles are much smaller (4 μm at 550 kHz vs 170 μm at 20 kHz),[15,42,43] thus considerably limiting the undesirable effects of shock waves on catalyst stability. To assess the stability of CuO_{HFUS} during the ultrasonic irradiation at a high frequency, the CuO_{HFUS} was filtered out at the end of the reaction and reused as collected without any further purification. As anticipated, the CuO_{HFUS} catalyst was found to be stable and was successfully recycled at least five times, without any appreciable decrease of the glucuronic acid yield, confirming that abrasion of CuO_{HFUS} was drastically limited under HFUS (Figure 6). SEM analysis of the spent CuO_{HFUS} catalyst showed no drastic change in morphology in comparison to the fresh catalysts (Figure S7c).

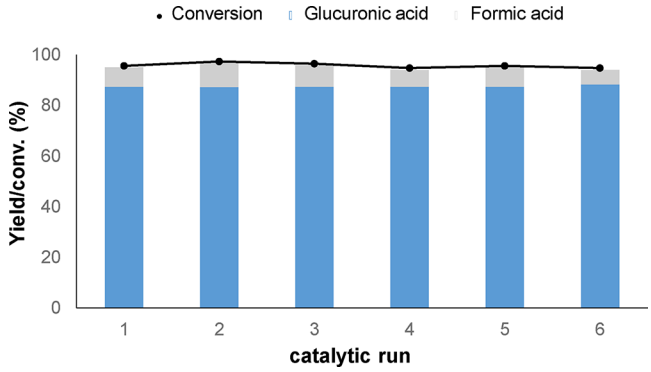

Figure 6. Recyling of CuO_{HFUS} (80 °C, 550 kHz, 10 wt % CuO_{HFUS}, glucose concentration 20 $g{\cdot}L^{-1}$, P_{acoust} = 0.36 $W{\cdot}mL^{-1}$).

CONCLUSION

We have provided theoretical and experimental evidence for an alternative reaction pathway provided by synergistic cavitation–copper oxide catalyst interactions. That is, H· and ·OH radicals generated during cavitation bubble implosions in water are diffused onto the surface of the CuO catalyst and selectively promote the oxidation of glucose to glucuronic acid under argon, in contrast to the gluconic acid formation in homogeneous bulk liquid solution. Through a combined experimental–theoretical approach, we showed that H· radical formed in situ by sonolysis of water are trapped by the surface lattice oxygen of CuO, making the ring-opening of glucose energetically unfavorable. Instead, the reaction takes an alternative pathway oriented to the selective oxidation of glucose to glucuronic acid, a valuable chemical whose synthesis remains a formidable scientific challenge in the field of catalysis. These results, providing first-hand insight into the participatory role of H· in the overall oxidation mechanism, also open a scientific line of thought on the unexplained role of

DOI: 10.1021/jacs.9b06824
J. Am. Chem. Soc. 2019, 141, 14772–14779

the atmosphere (O_2 vs Ar) previously observed on the catalyst-free oxidation of glucose assisted by ultrasound.[25] This aspect is the topic of current investigations in our groups.

From a more general point of view, this work demonstrates the general concept that the insertion of a solid catalyst during ultrasonic irradiation of organic solutes at a high frequency allows in situ radical reactions to be finely controlled. It also points toward a path to optimize the size of the catalyst for an ultrasonic frequency, which minimizes the damage to the catalyst resulting in reusable catalyst.

EXPERIMENTAL SECTION

Preparation of Copper(II) Oxide Nanoleaves under Low-Frequency Ultrasound Irradiation. All chemical reagents were used without further purification. In a typical synthesis method, 40 mL of 0.25 M NaOH aqueous solution was added to 10 mL of 0.5 M $Cu(NO_3)_2$ aqueous solution, and a sky-blue suspension was obtained. This suspension was subsequently exposed to a low-frequency ultrasound irradiation (19.95 kHz). Ultrasound was generated by a Digital Sonifier S-250D from Branson (power of standby P_0 = 27.0 W, nominal electric power of the generator P_{elec} = 8.2 W). A 3.2 nm diameter tapered microtip probe operating at a frequency of 19.95 kHz was used. The volume acoustic power of this system was $P_{acous.vol}$ = 0.25 W·mL^{-1} in water (determined by calorimetry measurements).[44] The ultrasound probe was immersed directly in the reaction medium and a minichiller cooler (Huber) was used to control the reaction temperature at 25 °C. On completion of sonication at the desired time, the dark brown precipitates were washed thoroughly with distilled water and dried in an oven at 60 °C overnight.

Preparation of Copper(II) Oxide Nanoleaves under High-Frequency Ultrasound Irradiation. All chemical reagents were used without further purification. In a typical synthesis method, 40 mL of 0.25 M NaOH aqueous solution was added to 10 mL of 0.5 M $Cu(NO_3)_2$ aqueous solution, and a sky-blue suspension was obtained. This suspension was subsequently subjected to an ultrasonic irradiation at high frequency (550 kHz) and at a controlled temperature of 40 °C (standby power P_0 = 13.9 W, nominal electric power of the generator P_{elec} = 70.4 W), with an acoustic power in water of $P_{acous.vol}$ = 0.44 W·mL^{-1} determined by calorimetry.[44] A minichiller cooler (Huber) was used to control the reaction temperature at 25 °C. On completion of sonication at the desired time, the dark brown precipitates were washed thoroughly with distilled water and dried in an oven at 60 °C overnight.

Sample Characterization. The as-synthesized CuO morphology was studied by SEM (JEOL JSM 6700F field emission), TEM, and high-resolution TEM (HR-TEM) (JEOLJEM-2100F). In each run, ∼50 mg of the catalyst was pretreated at 300 °C under a flow of He (30 mL min^{-1}) and then heated to 700 °C with a ramp of 10 °C min^{-1} in the stream of 5 vol % H_2/Ar (40 mL min^{-1}). Surface area analysis was determined by nitrogen physisorption on a Micromeritics TrisStar apparatus. The specific area was calculated using the Brunauer−Emmett−Teller (BET) equation. Crystallographic analyses were performed by means of XRD measurements in 2Θ mode on a Bruker AXS D8diffractometer with Cu Kα (=0.154056 Å) radiation at 40 kV and 20 mA. X-ray photoelectron spectrometry (XPS) was performed on a Thermo Escalab 250 spectrometer. The binding energy was calibrated using C 1s (284.6 eV) as a reference.

Carbohydrates Oxidation. Oxidation of glucose (or fructose, mannose, or galactose) was carried out in a 250 mL high-frequency ultrasonic reactor (SinapTec Ultrasonic Technology, NextGen Lab 1000). Typically, 2.0 g of glucose in 100 mL of distilled water was subjected to high-frequency ultrasound irradiation at a controlled temperature of 25 °C and a frequency of 550 kHz (standby power P_0 = 13.9 W, nominal electric power of the generator P_{elec} = 46.1 W), with an acoustic power in water of $P_{acous.vol}$ = 0.36 W·mL^{-1} determined by calorimetry using the procedure described in the literature.[44]

Product Analysis. Glucose and fructose were analyzed using a Shimadzu HPLC equipped with a pump system (LC-20AD), an autosampler SIL-10A, a controller CBM 20A, a refractive index detector from Waters, and a Zorbax NH_2 column (250 ± 4.6 mm). A mixture acetonitrile/water (20:80) was used as a mobile phase (0.4 mL min^{-1}). Glucuronic acid and other acid products were detected and quantified from the HPLC analysis by using the Varian Pro Star HPLC equipped with an ICE-COREGEL 107H column 300 × 7.8 mm from Transgenomic, a UV/vis detector (Varian Pro Star, 210 nm), and a refractive index detector (Varian 356-LC). A H_2SO_4 aqueous solution was used as the eluent with 0.4 mL·min^{-1} flow rate. External calibration of liquid chromatography was performed using standards of glucose, fructose, gluconic, formic, and glucuronic acid and was quantified by the difference between the two high-performance liquid chromatography (HPLC) analyses.

Density Functional Theory Details. All the intermediate transition states species as well as the free radicals including OH$^\bullet$ and $H_3O^\bullet$ involved in the ring-opening reaction of glucose have been calculated by using Gaussian 16 RevA.03 package[26] in the vacuum at the M05-2X/6-311++G(d,p) level of theory.[25] The M05-2X functional combined with the 6-311++G(d,p) basis set was proved to provide the best accuracy of the radical-molecule reaction including the H atom transfer, especially the barrier-less reaction with reactive radical like OH$^\bullet$.[45] The influence of the empirical dispersion corrections on the energy barriers was also taken into account using Grimme's D3 corrections.[46] All the intermediate compounds (Int) and transition states (TS) were identified by the number of imaginary frequencies (0 or 1, respectively). The intrinsic reaction coordinate (IRC) calculations were also performed to verify if the TSs were well-connected with the intermediate compounds. All the relative energies on the potential energy profiles are calculated in compared with the initial reactant, i.e., glucose.

All first-principles calculations for adsorptions and reactions on CuO(111) surface are performed based on periodic boundary conditions and plane-wave pseudopotential implementation of density functional theory (DFT) using the Vienna ab initio simulation package (VASP) developed at the Fakultät für Physik of the Universität Wien.[32,33] Projector augmented wave (PAW) method[47] employed with Perdew−Burke−Ernzerhof (PBE) exchange-correlation functional[48] is used to describe the interaction between valence electrons and ions with a plane-wave cutoff energy of 450 eV. We used a k-points sampling of 3 × 3 × 1 with Monkhorst−Pack scheme for integration over the Brillouin zone in reciprocal space and spin polarization is turned on for all simulations. The generalized gradient approximation (GGA) and the Hubbard correction U = 4.5 eV within the GGA+U scheme was used to correct the electron delocalization that occurs in strongly correlated systems such as transition metal oxides.[34,49,50] The optimized lattice parameters for CuO with GGA +U method are a = 4.5597 Å, b = 3.6059 Å, c = 5.1782 Å, and β = 96.3385°, which also matches very well with reported experimental data.[8] CuO catalyst is modeled by using the structure of p(4 × 2) slab of the most stable CuO(111) surface with 4 layers, and the vacuum thickness of 15 Å above the topmost layer was employed to avoid interactions between repeted slabs.[34] The bulklike magnetic configuration was reported to be the most stable arrangement for CuO(111) surface and, therefore, was used for all calculations in this study.[51] We do not use the dispersion correction within the GGA+U scheme because the inclusion of dispersion correction was reported to have only a small influence on the activation barriers for surface reations.[52] Furthermore, the inclusion of dispersion correction also worsens the performance of GGA+U method in predicting other surface properties (details are presented in the Supporting Information). Geometries were fully relaxed using the conjugate-gradient algorithm until the energy changed by <0.1 kJ/mol. Transition states were located using the climbing-nudged elastic band (Cl-NEB) method,[53] and frequency calculations confirmed the nature of the transition states with only one imaginary vibrational frequency.

DOI: 10.1021/jacs.9b06824
J. Am. Chem. Soc. 2019, 141, 14772−14779

■ ASSOCIATED CONTENT

Supporting Information

The Supporting Information is available free of charge on the ACS Publications website at DOI: 10.1021/jacs.9b06824.

CuO characterization before and after reaction, effect of catalyst loading, kinetic profile from fructose, characterization of the crude glucuronic acid, and additional information on DFT (PDF)

■ AUTHOR INFORMATION

Corresponding Authors

*mpsherb@berkeley.edu

*francois.jerome@univ-poitiers.fr

ORCID

Quang Thang Trinh: 0000-0002-3311-4691

Karine De Oliveira Vigier: 0000-0003-3613-7992

Duy Quang Dao: 0000-0003-0896-5168

Matthew P. Sherburne: 0000-0002-3992-1822

François Jérôme: 0000-0002-8324-0119

Author Contributions

○P.N.A. and Q.T.T. contributed equally.

Notes

The authors declare no competing financial interest.

■ ACKNOWLEDGMENTS

P.N.A., K.D.O.V., and F.J. are grateful to the CNRS, the University of Poitiers, and the Région Nouvelle Aquitaine for financial support. The International Consortium on Eco-conception and Renewable Resources (FR CNRS INCREASE 3707) and the chair "TECHNOGREEN" are also acknowledged for their funding. Q.T.T. and M.P.S. acknowledge the financial support by the National Research Foundation (NRF), Prime Minister's Office, Singapore under its Campus for Research Excellence and Technological Enterprise (CREATE) program. The computational work for this research was performed with resources of the National Supercomputing Centre, Singapore (NSCC). D.Q.D. is also indebted to the Centre de Ressources Informatiques (CRI) of the University of Lille and the Centre Régional Informatique et d'Applications Numériques de Normandie (CRIANN) for providing computer time of the theoretical calculations.

■ REFERENCES

(1) Michal, G.; Schomburg, D. *Biochemical pathways: an atlas of biochemistry and molecular biology*; Wiley: New York, 1999.

(2) Röper, H. Selective Oxidation of D-Glucose: Chiral Intermediates for Industrial Utilization. *Starch-Stärke* **1990**, *42* (9), 342−349.

(3) Amaniampong, P. N.; Li, K.; Jia, X.; Wang, B.; Borgna, A.; Yang, Y. Titania-Supported Gold Nanoparticles as Efficient Catalysts for the Oxidation of Cellobiose to Organic Acids in Aqueous Medium. *ChemCatChem* **2014**, *6*, 2105−2114.

(4) Amaniampong, P. N.; Jia, X.; Wang, B.; Mushrif, S. H.; Borgna, A.; Yang, Y. Catalytic oxidation of cellobiose over TiO2 supported gold-based bimetallic nanoparticles. *Catal. Sci. Technol.* **2015**, *5*, 2393−2405.

(5) Amaniampong, P. N.; Trinh, Q. T.; Li, K.; Mushrif, S. H.; Hao, Y.; Yang, Y. Porous structured CuO-CeO2 nanospheres for the direct oxidation of cellobiose and glucose to gluconic acid. *Catal. Today* **2018**, *306*, 172−182.

(6) Amaniampong, P. N.; Booshehri, A. Y.; Jia, X.; Dai, Y.; Wang, B.; Mushrif, S. H.; Borgna, A.; Yang, Y. High-temperature reduction improves the activity of rutile TiO2 nanowires-supported gold-copper bimetallic nanoparticles for cellobiose to gluconic acid conversion. *Appl. Catal., A* **2015**, *505*, 16−27.

(7) An, D.; Ye, A.; Deng, W.; Zhang, Q.; Wang, Y. Selective Conversion of Cellobiose and Cellulose into Gluconic Acid in Water in the Presence of Oxygen, Catalyzed by Polyoxometalate-Supported Gold Nanoparticles. *Chem. - Eur. J.* **2012**, *18*, 2938−2947.

(8) Amaniampong, P. N.; Trinh, Q. T.; Wang, B.; Borgna, A.; Yang, Y.; Mushrif, S. H. Biomass Oxidation: Formyl C-H Bond Activation by the Surface Lattice Oxygen of Regenerative CuO Nanoleaves. *Angew. Chem., Int. Ed.* **2015**, *54*, 8928−8933.

(9) Fel'dman, D.; Voitenko, A.; Shimanskaya, M.; Lidak, M. Y. Methods of obtaining D-glucuronic acid from D-glucose. II. Synthesis of glucuronides and their conversion into D-glucuronic acid. *Pharm. Chem. J.* **1983**, *17*, 134−140.

(10) Mehltretter, C.; Alexander, B.; Mellies, R.; Rist, C. A Practical Synthesis of D-Glucuronic Acid through the Catalytic Oxidation of 1, 2-Isopropylidene-D-glucose. *J. Am. Chem. Soc.* **1951**, *73*, 2424−2427.

(11) Mehltretter, C. The chemical synthesis of D-glucuronic acid. In *Advances in carbohydrate chemistry*; Elsevier: 1953; Vol. *8*, pp 231−249.

(12) Wojcieszak, R.; Cuccovia, I. M.; Silva, M. A.; Rossi, L. M. Selective oxidation of glucose to glucuronic acid by cesium-promoted gold nanoparticle catalyst. *J. Mol. Catal. A: Chem.* **2016**, *422*, 35−42.

(13) Marioli, J. M.; Kuwana, T. Electrochemical characterization of carbohydrate oxidation at copper electrodes. *Electrochim. Acta* **1992**, *37*, 1187−1197.

(14) Torto, N. Recent progress in electrochemical oxidation of saccharides at gold and copper electrodes in alkaline solutions. *Bioelectrochemistry* **2009**, *76*, 195−200.

(15) Suslick, K. S. Sonochemistry. *Science* **1990**, *247*, 1439−1445.

(16) Mahamuni, N. N.; Adewuyi, Y. G. Advanced oxidation processes (AOPs) involving ultrasound for waste water treatment: a review with emphasis on cost estimation. *Ultrason. Sonochem.* **2010**, *17*, 990−1003.

(17) Suslick, K. S.; Price, G. J. Applications of ultrasound to materials chemistry. *Annu. Rev. Mater. Sci.* **1999**, *29*, 295−326.

(18) Rinsant, D.; Chatel, G.; Jérôme, F. Efficient and Selective Oxidation of D-Glucose into Gluconic acid under Low-Frequency Ultrasonic Irradiation. *ChemCatChem* **2014**, *6*, 3355−3359.

(19) Shchukin, D. G.; Skorb, E.; Belova, V.; Möhwald, H. Ultrasonic cavitation at solid surfaces. *Adv. Mater.* **2011**, *23*, 1922−1934.

(20) Zhang, L.; Belova, V.; Wang, H.; Dong, W.; Möhwald, H. Controlled cavitation at nano/microparticle surfaces. *Chem. Mater.* **2014**, *26*, 2244−2248.

(21) Leighton, T. *The acoustic bubble*; Academic Press: 2012.

(22) Skorb, E. V.; Fix, D.; Shchukin, D. G.; Möhwald, H.; Sviridov, D. V.; Mousa, R.; Wanderka, N.; Schäferhans, J.; Pazos-Pérez, N.; Fery, A.; et al. Sonochemical formation of metal sponges. *Nanoscale* **2011**, *3*, 985−993.

(23) Amaniampong, P. N.; Karam, A.; Trinh, Q. T.; Xu, K.; Hirao, H.; Jérôme, F.; Chatel, G. Selective and Catalyst-free Oxidation of D-Glucose to D-Glucuronic acid induced by High-Frequency Ultrasound. *Sci. Rep.* **2017**, *7*, 40650.

(24) Amaniampong, P. N.; Trinh, Q. T.; Varghese, J. J.; Behling, R.; Valange, S.; Mushrif, S. H.; Jérôme, F. Unraveling the mechanism of the oxidation of glycerol to dicarboxylic acids over a sonochemically synthesized copper oxide catalyst. *Green Chem.* **2018**, *20*, 2730−2741.

(25) Zhao, Y.; Schultz, N. E.; Truhlar, D. G. Design of Density Functionals by Combining the Method of Constraint Satisfaction with Parametrization for Thermochemistry, Thermochemical Kinetics, and Noncovalent Interactions. *J. Chem. Theory Comput.* **2006**, *2*, 364−382.

(26) Frisch, M. J.; Trucks, G. W.; Schlegel, H. B.; Scuseria, G. E.; Robb, M. A.; Cheeseman, J. R.; Scalmani, G.; Barone, V.; Petersson, G. A.; Nakatsuji, H.; Li, X.; Caricato, M.; Marenich, A. V.; Bloino, J.; Janesko, B. G.; Gomperts, R.; Mennucci, B.; Hratchian, H. P.; Ortiz, J. V.; Izmaylov, A. F.; Sonnenberg, J. L.; Williams-Young, D.; Ding, F.; Lipparini, F.; Egidi, F.; Goings, J.; Peng, B.; Petrone, A.; Henderson, T.; Ranasinghe, D.; Zakrzewski, V. G.; Gao, J.; Rega, N.; Zheng, G.;

DOI: 10.1021/jacs.9b06824
J. Am. Chem. Soc. 2019, 141, 14772−14779

Liang, W.; Hada, M.; Ehara, M.; Toyota, K.; Fukuda, R.; Hasegawa, J.; Ishida, M.; Nakajima, T.; Honda, Y.; Kitao, O.; Nakai, H.; Vreven, T.; Throssell, K.; Montgomery, Jr., J. A.; Peralta, J. E.; Ogliaro, F.; Bearpark, M. J.; Heyd, J. J.; Brothers, E. N.; Kudin, K. N.; Staroverov, V. N.; Keith, T. A.; Kobayashi, R.; Normand, J.; Raghavachari, K.; Rendell, A. P.; Burant, J. C.; Iyengar, S. S.; Tomasi, J.; Cossi, M.; Millam, J. M.; Klene, M.; Adamo, C.; Cammi, R.; Ochterski, J. W.; Martin, R. L.; Morokuma, K.; Farkas, O.; Foresman, J. B.; Fox, D. J. *Gaussian 16, Rev. B.01*; Gaussian, Inc.: Wallingford, CT, 2016.

(27) Bhola, K.; Varghese, J. J.; Dapeng, L.; Liu, Y.; Mushrif, S. H. Influence of Hubbard U Parameter in Simulating Adsorption and Reactivity on CuO: Combined Theoretical and Experimental Study. *J. Phys. Chem. C* **2017**, *121*, 21343−21353.

(28) Maimaiti, Y.; Nolan, M.; Elliott, S. D. Reduction mechanisms of the CuO(111) surface through surface oxygen vacancy formation and hydrogen adsorption. *Phys. Chem. Chem. Phys.* **2014**, *16*, 3036−3046.

(29) Varghese, J. J.; Trinh, Q. T.; Mushrif, S. H. Insights into the synergistic role of metal−lattice oxygen site pairs in four-centered C−H bond activation of methane: the case of CuO. *Catal. Sci. Technol.* **2016**, *6*, 3984−3996.

(30) Singuru, R.; Trinh, Q. T.; Banerjee, B.; Govinda Rao, B.; Bai, L.; Bhaumik, A.; Reddy, B. M.; Hirao, H.; Mondal, J. Integrated Experimental and Theoretical Study of Shape-Controlled Catalytic Oxidative Coupling of Aromatic Amines over CuO Nanostructures. *ACS Omega* **2016**, *1*, 1121−1138.

(31) Song, Y.-Y.; Wang, G.-C. A DFT Study and Microkinetic Simulation of Propylene Partial Oxidation on CuO(111) and CuO(100) Surfaces. *J. Phys. Chem. C* **2016**, *120*, 27430−27442.

(32) Kresse, G.; Furthmüller, J. Efficiency of ab-initio total energy calculations for metals and semiconductors using a plane-wave basis set. *Comput. Mater. Sci.* **1996**, *6*, 15−50.

(33) Kresse, G.; Hafner, J. Ab initio molecular dynamics for liquid metals. *Phys. Rev. B: Condens. Matter Mater. Phys.* **1993**, *47*, 558−561.

(34) Trinh, Q. T.; Bhola, K.; Amaniampong, P. N.; Jérôme, F.; Mushrif, S. H. Synergistic Application of XPS and DFT to Investigate Metal Oxide Surface Catalysis. *J. Phys. Chem. C* **2018**, *122*, 22397−22406.

(35) Trinh, Q. T.; Chethana, B. K.; Mushrif, S. H. Adsorption and Reactivity of Cellulosic Aldoses on Transition Metals. *J. Phys. Chem. C* **2015**, *119*, 17137−17145.

(36) Mushrif, S. H.; Varghese, J. J.; Vlachos, D. G. Insights into the Cr(iii) catalyzed isomerization mechanism of glucose to fructose in the presence of water using ab initio molecular dynamics. *Phys. Chem. Chem. Phys.* **2014**, *16*, 19564−19572.

(37) Nørskov, J. K.; Studt, F.; Abild-Pedersen, F.; Bligaard, T. Rate Constants. In *Fundamental Concepts in Heterogeneous Catalysis*; Nørskov, J. K., Studt, F., Abild-Pedersen, F., Bligaard, T., Eds.; Wiley: 2014.

(38) Trinh, Q. T.; Banerjee, A.; Yang, Y.; Mushrif, S. H. Sub-Surface Boron-Doped Copper for Methane Activation and Coupling: First-Principles Investigation of the Structure, Activity, and Selectivity of the Catalyst. *J. Phys. Chem. C* **2017**, *121*, 1099−1112.

(39) Zope, B. N.; Hibbitts, D. D.; Neurock, M.; Davis, R. J. Reactivity of the Gold/Water Interface During Selective Oxidation Catalysis. *Science* **2010**, *330*, 74−78.

(40) Yoo, J. S.; Khan, T. S.; Abild-Pedersen, F.; Nørskov, J. K.; Studt, F. On the role of the surface oxygen species during A−H (A = C, N, O) bond activation: a density functional theory study. *Chem. Commun.* **2015**, *51*, 2621−2624.

(41) Tauber, A.; Mark, G.; Schuchmann, H.-P.; von Sonntag, C. Sonolysis of tert-butyl alcohol in aqueous solution. *J. Chem. Soc., Perkin Trans. 2* **1999**, 1129−1136.

(42) Suslick, K. S. *Ultrasound: its chemical, physical, and biological effects*; VCH Verlagsgesellschaft: Weinheim, Germany, 1988.

(43) McKenzie, T. G.; Karimi, F.; Ashokkumar, M.; Qiao, G. G. Ultrasound and Sonochemistry for Radical Polymerization: Sound Synthesis. *Chem. - Eur. J.* **2019**, *25*, 5372−5388.

(44) Koda, S.; Kimura, T.; Kondo, T.; Mitome, H. A standard method to calibrate sonochemical efficiency of an individual reaction system. *Ultrason. Sonochem.* **2003**, *10*, 149−156.

(45) Galano, A.; Alvarez-Idaboy, J. R. Kinetics of radical-molecule reactions in aqueous solution: A benchmark study of the performance of density functional methods. *J. Comput. Chem.* **2014**, *35*, 2019−2026.

(46) Grimme, S. Density functional theory with London dispersion corrections. *WIREs Comput. Mol. Sci.* **2011**, *1*, 211−228.

(47) Blöchl, P. E. Projector augmented-wave method. *Phys. Rev. B: Condens. Matter Mater. Phys.* **1994**, *50*, 17953−17979.

(48) Perdew, J. P.; Burke, K.; Ernzerhof, M. Generalized Gradient Approximation Made Simple. *Phys. Rev. Lett.* **1996**, *77*, 3865−3868.

(49) Dudarev, S. L.; Botton, G. A.; Savrasov, S. Y.; Humphreys, C. J.; Sutton, A. P. Electron-energy-loss spectra and the structural stability of nickel oxide: An LSDA+U study. *Phys. Rev. B: Condens. Matter Mater. Phys.* **1998**, *57*, 1505−1509.

(50) Anisimov, V. I.; Zaanen, J.; Andersen, O. K. Band theory and Mott insulators: Hubbard U instead of Stoner I. *Phys. Rev. B: Condens. Matter Mater. Phys.* **1991**, *44*, 943−954.

(51) Hu, J.; Li, D.; Lu, J. G.; Wu, R. Effects on Electronic Properties of Molecule Adsorption on CuO Surfaces and Nanowires. *J. Phys. Chem. C* **2010**, *114*, 17120−17126.

(52) Trinh, Q. T.; Nguyen, A. V.; Huynh, D. C.; Pham, T. H.; Mushrif, S. H. Mechanistic insights into the catalytic elimination of tar and the promotional effect of boron on it: first-principles study using toluene as a model compound. *Catal. Sci. Technol.* **2016**, *6*, 5871−5883.

(53) Henkelman, G.; Uberuaga, B. P.; Jónsson, H. A climbing image nudged elastic band method for finding saddle points and minimum energy paths. *J. Chem. Phys.* **2000**, *113*, 9901−9904.

DOI: 10.1021/jacs.9b06824
J. Am. Chem. Soc. 2019, 141, 14772−14779